Check for updates

Seven new mutations in the nicotinamide adenine dinucleotide reduced–cytochrome b_5 reductase gene leading to methemoglobinemia type I

Jan Dekker, Michel H. M. Eppink, Rob van Zwieten, Thea de Rijk, Angel F. Remacha, Lap Kay Law, Albert M. Li, Kam Lau Cheung, Willem J. H. van Berkel, and Dirk Roos

Cytochrome b_5 reductase (b5R) deficiency manifests itself in 2 distinct ways. In methemoglobinemia type I, the patients only suffer from cyanosis, whereas in type II, the patients suffer in addition from severe mental retardation and neurologic impairment. Biochemical data indicate that this may be due to a difference in mutations, causing enzyme instability in type I and complete enzyme deficiency or enzyme inactivation in type II. We have investigated 7 families with methemoglobulinemia type I and found 7 novel mutations in the *b5R* gene. Six of these mutations predicted amino acid substitutions at sites not involved in reduced nicotinamide adenine dinucleotide (NADH) or flavin adenine dinucleotide (FAD) binding, as deduced from a 3-dimensional model of human b5R. This model was constructed from comparison with the known 3-dimensional structure of pig b5R. The seventh mutation was a splice site mutation leading to skipping of exon 5 in messenger RNA, present in heterozygous form in a patient together with a missense mutation on the other allele. Eight other amino acid substitutions, previously described to cause methemoglobinemia type I, were also situated in nonessential regions of the enzyme. In contrast, 2 other substitutions, known to cause the type II form of the disease, were found to directly affect the consensus FAD-binding site or indirectly influence NADH binding. Thus, these data support the idea that enzyme inactivation is a cause of the type II disease, whereas enzyme instability may lead to the type I form. (Blood. 2001;97: 1106-1114)

© 2001 by The American Society of Hematology

Introduction

Nicotinamide adenine dinucleotide reduced (NADH) cytochrome b_5 reductase (b5R; EC 1.6.2.2) is a 300–amino acid, membrane-bound enzyme localized in the endoplasmic reticulum of all tissue cells. This enzyme transfers electrons from NADH to cytochrome b_5 via its flavin adenine dinucleotide (FAD) prosthetic group.[1] Reduced cytochrome b_5 then donates its electrons to various acceptors involved in elongation and desaturation of fatty acids, cholesterol biosynthesis, and cytochrome P-450–mediated drug metabolism.[2-5] In erythrocytes, a 25–amino acid shorter, soluble form of b5R exists, which is functional in methemoglobin reduction.[6,7] Both forms of b5R are derived from a single gene,[8] but recent studies have indicated that an erythroid-specific transcript generates the soluble form of b5R in humans.[9]

The primary structure of b5R is highly conserved among mammalian species.[10] The 31-kd hydrophilic form of the human enzyme shows 92% sequence identity with the solubilized form of pig liver b5R, for which a 3-dimensional model of the crystal structure (1ndh) at 2.4 Å resolution is available.[11] A preliminary account of the molecular structure of the human enzyme at 2.5 Å has also been published.[12] The crystallographic analysis has revealed that 1ndh consists of 2 domains that are separated by a large interdomain cleft. The N-terminal domain, which harbors the FAD, is structurally related to the FAD-binding domain of ferredoxin-$NADP^+$ reductase (FNR).[13] The C-terminal domain of 1ndh is involved in NADH binding, and its structure is somewhat different from the corresponding FNR domain. Despite the presence of a Rossmann fold[14] and the structural homology with several other flavoenzymes,[15-25] the exact mode of NADH binding in 1ndh is unknown. Nevertheless, it has been suggested that the large interdomain cleft permits the nicotinamide moiety of NADH to access the *re* side of the isoalloxazine ring of the flavin without a conformational change of the C-terminal region.[11] This would be different from the situation in FNR, where a displacement of a tyrosine residue is required for direct hydride transfer from NADPH to FAD.[21,26]

Deficiency of b5R may lead to 2 different clinical phenotypes. In type I methemoglobulinemia, cyanosis is the only clinical symptom.[27,28] In type II methemoglobulinemia, cyanosis is accompanied by severe mental retardation and neurologic impairment.[29,30] In type I, the b5R enzyme deficiency is profound in the erythrocytes ($<$ 10% of normal activity) and moderate in other blood and tissue cells (20%-60% of normal activity).[31-34] In type II, the b5R deficiency is generalized to all tissues.

The human b5R gene *DIA1* is localized at chromosome 22q13 and contains 9 exons.[8] Until now, 7 different mutations in this gene have been described to lead to type I b5R deficiency,[33-39] and 11 different mutations to the type II disease.[31,32,34,40-44] In general, type I mutations were found in "marginal portions" of the enzyme,

From the Central Laboratory of the Netherlands Blood Transfusion Service (CLB), and Laboratory for Experimental and Clinical Immunology, Academic Medical Center, University of Amsterdam, Amsterdam, and Department of Biomolecular Sciences, Laboratory of Biochemistry, Wageningen University, Wageningen, The Netherlands; Hospital de la Santa Creu I Sant Pau, Barcelona, Spain; Departments of Chemical Pathology and Paediatrics, Prince of Wales Hospital, Shatin, NT, Hong Kong.

Submitted July 26, 2000; accepted October 19, 2000.

Reprints: Dirk Roos, Central Laboratory Netherlands Blood Transfusion Service, Plesmanlaan 125, 1066CX Amsterdam, The Netherlands; e-mail: d_roos@clb.nl.

The publication costs of this article were defrayed in part by page charge payment. Therefore, and solely to indicate this fact, this article is hereby marked "advertisement" in accordance with 18 U.S.C. section 1734.

© 2001 by The American Society of Hematology

Downloaded from http://ashpublications.net/blood/article-pdf/97/4/1106/1671579/h8040101106.pdf by guest on 02 June 2024

Table 1. Sequences of the primers used for amplification of the *b5R* gene

Exon and primer/fragment code	Direction (sense or antisense)	Primers	Amplimer length (bp)
FLAG	—	5′ TGT AAA ACG ACG GCC AGT 3′	—
Exon 1	S	5′ FLAG + CAG AAG CAG GCG GAG CGA CC 3′	252
E1	AS	5′ GTC CCA GTC CCT CGC GAC GC 3′	
Exon 2	S	5′ FLAG + TAG TGT GGA CAA GAA GCC GGT GT 3′	310
E2	AS	5′ TAC TTC AGA GCA GAC CAT GC 3′	
Exon 3	AS	5′ FLAG + ACG TCC CAG CTT CCT GCC TC 3′	352
E3	S	5′ CGT TCA GCA GCT TTG GGC C 3′	
Exon 4	S	5′ FLAG + GCA CCA GCA GGA GTG AAG GCA 3′	363
E4	AS	5′ CAC CCA CAC CCC CTC CAC AG 3′	
Exon 5	S	5′ FLAG + TGC AGA AGA GGC ACT TGT CC 3′	268
E5	AS	5′ GTG TAA CCA AGG GAT TCC GA 3′	
Exon 6	S	5′ FLAG + CCG GGC CTC ACC CCT TCT C 3′	473
E6/7	AS	5′ CAG GGT AAG CTG AGT TTC CC 3′	
Exon 7	AS	5′ FLAG + CAG GGT AAG CTG AGT TTC CC 3′	473
E7/6	S	5′ CCG GGC CTC ACC CCT TCT C 3′	
Exon 8	S	5′ FLAG + TGA AAG CTC CGC AAG CGT GT 3′	327
E8	AS	5′ TCC AAA GCT CAA CGC CAC AA 3′	
Exon 9	S	5′ FLAG + GCA TTT AAG AAT TCA CCG CC 3′	354
E9	AS	5′ GGA GGT GAC TGG GTG AGC GT 3′	

giving rise to enzymatically active, but unstable proteins. Type II mutations cause exon skipping in messenger RNA (mRNA) and premature protein synthesis termination, or are localized in consensus FAD- or NADH-binding sites of b5R, leading to loss of protein expression or to expression of enzymatically inactive proteins. Due to the long half-life of erythrocytes and the lack of protein synthesis in these cells, type I b5R deficiency is mainly found in the red blood cells, whereas type II b5R deficiency is apparent in all tissue cells, with much more detrimental effects.

We now describe 7 new mutations in the b5R gene leading to type I methemoglobulinemia. These and previously published mutations were tested in a 3-dimensional structural model of human b5R for their effects on structure and function of b5R.

Patients, materials, and methods

Patients were classified as having methemoglobinemia when cyanosis was apparent, methemoglobin (metHb) in the blood was above 5% and/or metHb reductase in the erythrocytes was below 0.5 IU/g Hb. The patients were regarded to suffer from methemoglobinemia type I if neurologic abnormalities had not become manifest at the age of 6 to 9 months. EDTA or citrated blood samples were washed 3 times with 0.9% NaCl solution. MetHb reductase activity in the red cells was measured with the method of Hegesh and coworkers[45] in a Beckman DU-65 spectrophotometer (Beckman Coulter, Fullerton, CA). The metHb levels were measured by the method of Evelyn and Malloy[46] with a Hewlett Packard 8451A diode-array spectrophotometer or with an OSM3 Hemoximeter from Radiometer (Copenhagen, Denmark). A Puregene DNA isolation kit (Gentra Systems, Minneapolis, MN) was used to isolate DNA from leukocytes. RNA was isolated from leukocytes by the method of Chirgwin and colleagues,[47] followed by synthesis of complementary DNA (cDNA) as described by Bolscher and associates.[48]

DNA amplification and sequencing

Polymerase chain reaction (PCR) was performed in sealed glass capillaries containing 15 μL of reaction mixture consisting of 2 μL 10 × bovine serum albumin (BSA) solution (2.5 μg/μL BSA, Sigma Chemical, St Louis, MO), 1.5 μL Thermophilic DNA polymerase (Promega, Madison, WI) in 10 × buffer (100 mM Tris-HCl, pH 9.0, 500 mM KCl, 1% vol/vol Triton X-100), 0.75 μL $MgCl_2$ 25 mM, 0.6 μL dNTP solution (dATP, dCTP, dGTP, dTTP, 5 mM each; Gibco BRL, Gaithersburg, MD), 0.2 μL anti-Taq DNA polymerase (7 μM; 1.1 μg/μL in 50 mM KCl, 10 mM Tris-HCl, 50 vol % glycerol, pH 7.0; Clontech, Palo Alto, CA), 0.2 μL Taq DNA polymerase (5 U/μL; Promega), 0.5 μL flagged sense primer (10 μM) (Table 1), 1 μL antisense primer (10 μM) (Table 1), 5 μL genomic DNA solution (0.025 μg/μL in demineralized water) and filled up to 15 μL with demineralized water.

Exon 1 of the *b5R* gene is very GC-rich and was therefore amplified with the following adaptations: 0.45 μL $MgCl_2$ 25 mM, 0.6 μL 7-deaza-dNTP solution 75% (3.75 mM 7deaza-dGTP, 1.25 mM dGTP, 5 mM dATP, 5 mM dCTP, 5 mM dTTP; Boehringer Mannheim, Mannheim, Germany) and addition of 3 μL GC-melt (5 M GC-melt, Clontech).

The PCR equipment consisted of an Air Thermo Cycler (ATC) (type: 1605, Idaho Technology, Idaho Falls, ID).

The cycle conditions were denaturation 5 seconds at 96°C, annealing 20 seconds at 65°C, and elongation 20 seconds at 72°C, for 40 cycles. Fragments 5 and 6,7 had annealing temperatures of 62°C and 68°C, respectively. Fragment 1 had an annealing/elongation time of 80 seconds at 72°C and was amplified for 60 cycles.

The oligonucleotide flag on the forward PCR primers was complementary to the −21m13 forward fluorescent primer. Direct sequencing of the amplified products was performed with BigDye Primer Cycle Sequencing Ready Reaction kit −21m13 FWD from ABI Prism, (Applied Biosystems, Warrington, United Kingdom). For each of the bases deoxy-A, -C, -G or -T, 4 μL of "ready reaction-mix A or C or G or T," 1 μL of the 1:10 water-diluted PCR product, and 25 μL Biozym Biowax was put in a 96-well plate. The cycle sequence reactions were performed on PCR equipment from Hybaid (Middlesex, United Kingdom) type; OmniGene (Biozym, Landgraaf, The Netherlands) under the following conditions: denaturation 1 second at 95°C, annealing/elongation 15 seconds at 60°C, for 40 cycles. Subsequently, products of the same PCR sample were pooled and desalted with the Sephadex G-50/multiscreen system (Millipore, Molsheim, France) according to the Dye Terminator Removal protocol (http://www.millipore.com/analytical/technote/multiscreen/tn053/). The dried samples were dissolved in 3 μL sequence loading buffer (Amersham Pharmacia Biotech, Uppsala, Sweden). The samples were denatured for 2 minutes at 95°C, put on ice and loaded on an ABI Prism 377 sequencer (Applied Biosystems, Foster City, CA), run module settings: Seq Run 36E-1200, dRhoda matrix, DP 5%BD–21m13FWD. The sequencer was casted with a 5% acrylamide longranger-gel prepared from a 50% stock solution (FMC BioProducts, Vallensbeak Strand, Denmark).

Downloaded from http://ashpublications.net/blood/article-pdf/97/4/1106/1671579/h8040101106.pdf by guest on 02 June 2024

cDNA amplification and sequencing

The cDNA was amplified as was genomic DNA, with about 2 ng cDNA in 5 μL demineralized water. The primers used to amplify exons 4, 5, and 6 were sense 5′ GTGGGCCAGCACATCTACCT and antisense 5′ GATCATGCCCACGGACTTCA. The cycle conditions were denaturation 5 seconds at 96°C, annealing 20 seconds at 60°C, and elongation 30 seconds at 72°C, for 35 cycles at slope 9. Direct sequencing of the amplified products was performed with the BigDye Terminator cycle sequencing Ready Reaction kit (Applied Biosystems, no. 4303153). Four microliters of this reaction mixture, 4 μL demineralized water, 2 μL antisense primer (10 μM), 1 μL of the antisense product, and 25 μL Biowax (Biozym) were put in a 96-well polycarbonate plate. The cycle conditions were 2 seconds at 95°C and 2 minutes at 70°C for 35 cycles in an Omnigene Thermocycler (Hybaid) with simultaneous tube control and calibration factor 200. The sequencing samples were purified and loaded on an ABI Prism 377 sequencer (Applied Biosystems) as described for genomic DNA.

Restriction fragment analysis

Restriction fragment analysis was performed with the following enzymes.

*Nci*I (*Bcn*I) cuts after C′ in CC′GGG, indicative for the mutation G→A in exon 2 (R49Q; single-letter amino acid codes); the PCR product with the normal sequence will be digested.

*BsiE*I (*Bsh1285*I) cuts after G′ in CG′GCCG, indicative for the mutation C→T in exon 3 (P64L); the PCR product (made with a mismatch primer) with the normal sequence will be digested.

*Apa*I *(Bsp1201)* cuts after C[prime in GGGCC′C, indicative for the mutation C→T in exon 5 (L144P); the PCR product with the normal sequence will be digested.

*BstU*I (*Bsh1236*I) cuts after G′ in CG′CG, indicative for the mutation G→A in exon 6 (A178T); the PCR product with the normal sequence will be digested. With the same enzyme the T→G mutation in exon 8 (L238R) was tested; the PCR product with the mutated sequence will be digested.

*Pag*1 *(BspH*1*)* cuts after T′ in T′CATGA, indicative for the mutation G→A in exon 9 (V252M); the PCR product with the mutated sequence will be digested.

The assays were performed with 1 μL restriction enzyme, 1 μL restriction enzyme buffer, 4 μL demineralized water, and 5 μL of the PCR product. Digestion took place overnight at 37°C. The products were loaded on a 1% agarose gel with ethidium bromide and were run for 30 minutes at 100 mA.

Structure homology modeling

The globular fold of human b5R was predicted with MODELLER[49] using the CHARMM forcefield.[50] The 3-dimensional model of the crystal structure of pig liver b5R at 2.4 Å resolution (Brookhaven Protein Data Bank file: 1ndh; reference 11) served as the template file. The stereochemical quality of the homology model was verified by PROCHECK[51] and the protein folding was assessed with PROFILE[52] and PROSAII,[53] which evaluate the compatibility of each residue to its environment independently. After this initial verification, incompatible regions of the model were optimized with the simulated annealing procedure (molecular dynamics) of the XPLOR package,[54] thereby fixing the other parts of the protein. A simulated annealing calculation was performed for 1000 steps at 900 K, with each step taking 0.5 femtosecond. Before and after molecular dynamics the model was energy minimized with the conjugate gradient algorithm of XPLOR, the minimization converged after 2000 cycles (gradient: 0.1 kcal/mol). Again, the model was checked and verified. NADH docking was performed with the program O,[55] based on the mode of NADP(H) binding in the related structure of ferredoxin-NAD(P)$^+$ reductase.[26] NADH forcefield constants for energy minimization were derived from CHARMM. Finally, the model was verified after several rounds of energy minimization.

Results

Family studies

In family V, both parents showed half-normal metHb reductase activity, correlating with the G757A (exon 9) mutation in one of their alleles (Figure 1A, Table 2). This mutation leads to the replacement of Val to Met at position 252. The 2 affected children were homozygotes for the G757A mutation and showed almost no metHb reductase activity. Their brother lacked the mutation and was unaffected.

Family A had the same mutation as found in family V. Both parents as well as one child were heterozygotes. These 3 individuals showed decreased enzyme activity. The 2 patients in the family were homozygotes for the mutation, showed very low metHb reductase activity and had about 10% metHb in their red cells (Figure 1A, Table 2).

Mr T, whose relatives were not available for investigation, was a homozygote for the G757A mutation and had almost no metHb reductase activity (Figure 1A, Table 2). As far as we know, Mr T and the families V and A are not related to each other. In all 3 of these families, the mutation was confirmed by restriction analysis and was excluded as a polymorphism in 50 control DNA samples (100 alleles).

In family W, a C to T mutation in exon 5 was found by sequencing (Figure 1B). This C434T mutation predicts the substitution of a proline to leucine at position 144. Also this mutation was confirmed by restriction analysis. Unfortunately, we could not investigate the DNA of the presumably homozygous patient II.3 (Figure 2), because he died between the time of enzyme analysis and the time of DNA analysis. In his family members, the presence of the heterozygous C434T mutation correlated with a metHb reductase activity of half the control value (Table 2). The family members who lacked the mutation showed a normal metHb reductase activity, indicating that the C434T mutation was the cause of the enzyme deficiency.

Mutation C434T was excluded as a polymorphism in 50 control DNA samples (100 alleles). Only in one control sample, the exon 5 PCR product was not totally digested by *Apa*I. When this sample was further investigated by sequencing, it became clear that the enzyme was not capable of digesting one allele because a polymorphic C432T was present. The normal sequence is 429GGGCCC434; the C434T mutation leads to 429GGGCCT434 and the polymorphism to 429GGGTCC434. The metHb reductase activity of this variant sample was normal.

In family Am from Spain, we found (Figure 1C) the parents to be heterozygotes, each for a different mutation, viz. G149A (predicting substitution of arginine for glutamine at position 49 in exon 2) and C194T (predicting substitution of proline for leucine at position 64 in exon 3). Two of their children proved to be compound heterozygotes for these mutations. Only in child 1, a girl, this situation was manifested by 6% metHb, low metHb reductase activity, and slight cyanosis in her lips (Table 2). Child 2, her brother, had 2% metHb and half-normal metHb reductase activity, without clinical signs. The third child, a girl, proved to be a heterozygote for the G149A mutation and had low normal metHb reductase activity. The fourth child was enzymatically and genetically unaffected. These mutations were confirmed by restriction analysis and excluded as polymorphisms by analysis of 50 control DNA samples.

Family L from Hong Kong had an almost 2-month-old baby

Downloaded from http://ashpublications.net/blood/article-pdf/97/4/1106/1671579/h8040101106.pdf by guest on 02 June 2024

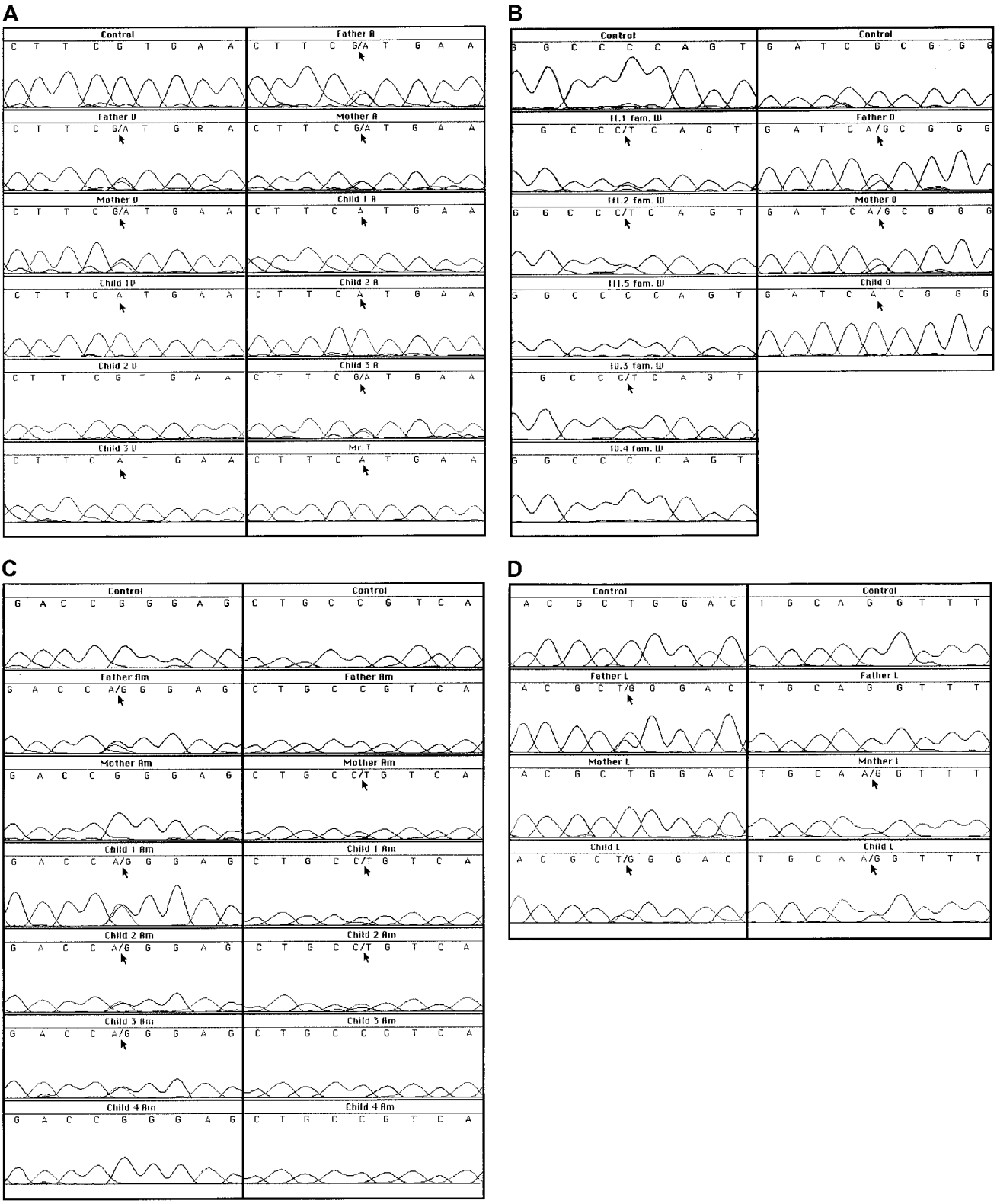

Figure 1. Sequence analyses of genomic DNA. (A) Results of a fragment around G757 in families V, A, and T. (B) Results of a fragment around C434 in family W and a fragment around G535 in family O. (C) Results of a fragment around G149 and a fragment around C194 in family Am. (D) Results of a fragment around T716 and a fragment around the intron 4/exon 5 boundary in family L.

with severe cyanosis. This patient had 9% metHb in her erythrocytes and very low metHb reductase activity (Table 2). The parents had half-normal metHb reductase activity. In exon 8 we found a T716G mutation heterozygous in the father and in the child (Figure 1D). This mutation predicts the substitution of a leucine to an arginine at position 238. In 50 control DNA samples, the T716G mutation was excluded as a polymorphism. In the child and in the mother, another mutation was found at the 3′ end of intron 4, where

Downloaded from http://ashpublications.net/blood/article-pdf/97/4/1106/1671579/h8040101106.pdf by guest on 02 June 2024

Table 2. Summary of results

Individual	MetHb (%)	MetHb reductase (IU/g Hb)	Mutation	Amino acid change
Healthy controls (n = 0)	< 1.0	1.7-3.5		
Family V				
Father	not tested	1.5	G757A heterozygote	V252M
Mother	not tested	1.3	G757A heterozygote	V252M
Child 1	not tested	0.1	G757A homozygote	V252M
Child 2	not tested	3.0	G757G normal	
Child 3	not tested	0	G757A homozygote	V252M
Family A				
Father	0.4	0.7	G757A heterozygote	V252M
Mother	0.4	1.0	G757A heterozygote	V252M
Child 1	10.7	0.1	G757A homozygote	V252M
Child 2	10.0	0.1	G757A homozygote	V252M
Child 3	0.5	1.5	G757A heterozygote	V252M
Family T				
Mr T	0.3	0.2	G757A homozygote	V252M
Family W				
II.1	0.4	1.2	C434T heterozygote	P144L
II.3	not tested	0	not tested	
II.4	not tested	1.2	not tested	
III.2	0.7	0.7	C434T heterozygote	P144L
III.3	not tested	0.5	not tested	
III.5	0.4	3.0	C434C normal	
IV.1	not tested	1.7	not tested	
IV.2	not tested	1.9	not tested	
IV.3	0.3	1.1	C434T heterozygote	P144L
IV.4	0.4	2.0	C434C normal	
IV.5	not tested	1.0	not tested	
Family Am				
Father	0.7	2.3	G149A heterozygote	R49Q
Mother	0.1	1.6	C194T heterozygote	P64L
Child 1	6.1	0.4	G149A heterozygote	R49Q
			C194T heterozygote	P64L
Child 2	2.0	0.8	G149A heterozygote	R49Q
			C194T heterozygote	P64L
Child 3	0.7	1.3	G149A heterozygote	R49Q
Child 4	not tested	2.6	normal	
Family L				
Father	2.8	1.1	T716G heterozygote	L238R
Mother	1.7	1.1	intron 4 − 1g → a heterozygote	Splice defect
Child	9.1	0.2	T716G heterozygote	L238R
			Intron 4 − 1g → a heterozygote	Splice defect
Family O				
Father	1.0	1.5	G535A heterozygote	A178T
Mother	2.0	1.1	G535A heterozygote	A178T
Child	31	0.1	G535A homozygote	A178T

Single-letter amino acid codes used.

the normal sequence cagGTTTAC was replaced on one allele by caaGTTTAC (Figure 1D). This acceptor splice site mutation predicts skipping of exon 5 during mRNA processing. Indeed, in the mother's cDNA the sequence of exon 4 was followed by a mixture of exon 5 and exon 6 sequences (not shown), indicating that she was heterozygous for a mutation that caused skipping of exon 5. From the child, no RNA or cDNA was available for these investigations. Both mutations in this family were confirmed by restriction analysis. The child showed no neurologic abnormalities at the age of 1 year.

In family O, of North African origin, a newborn girl presented with severe cyanosis. This patient had 31% metHb in her erythrocytes and very low metHb reductase activity (Table 2). In her DNA we found an apparently homozygous G535A mutation in exon 6 of the *DIA1* gene (Figure 1B), predicting an A178T substitution. Both parents proved to be heterozygous for this mutation; their metHb percentage was low and their metHb reductase activity was below the normal range (Figure 1B, Table 2). The G535A mutation was confirmed by restriction analysis and excluded as a polymorphism in 50 control DNA samples. The child showed no signs of neurologic abnormalities at the age of 9 months.

Structural properties

Figure 3 shows the sequence alignment of human b5R and the solubilized form of pig liver b5R. From this alignment it is obvious that both structures are highly homologous. The amino acid differences between both enzymes are spread throughout the structure and are mainly localized in flexible regions near the protein surface. None of the variable residues are directly involved in FAD or NADH binding.

Downloaded from http://ashpublications.net/blood/article-pdf/97/4/1106/1671579/h8040101106.pdf by guest on 02 June 2024

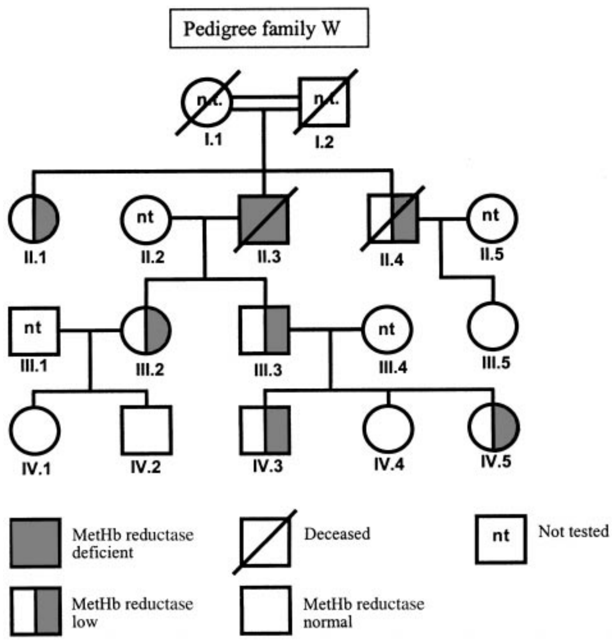

Figure 2. Pedigree of family W. See also Table 2.

A 3-dimensional model of the structure of human b5R was constructed, based on the crystal structure of the solubilized form of 1ndh. A ribbon diagram of the modeled structure of human b5R is presented in Figure 4. From this structural model and the sequence alignment, the location of the amino acid substitutions in b5R of the methemoglobinemia patients can be deduced (see "Discussion").

The NADH cofactor was modeled in an extended conformation, highly similar to the mode of binding of NADP(H) in the related ferredoxin $NADP^+$ reductase.[26] The NADH molecule is situated in the interdomain cleft at the *re* side of the FAD isoalloxazine ring (Figure 4).

Figure 3. Sequence alignment of membrane-bound human b5R with the solubilized form of pig liver b5R. Differences between the human and the pig enzyme are indicated by an asterisk. Secondary structure elements are underlined, the fingerprint sequence for binding the pyrophosphate moiety of NADH[56] is depicted in bold, and type I mutated residues are indicated by a shadowed box.

Figure 4. Ribbon diagram of the 3-dimensional model of the soluble form of human b5R. The crystal structure of the solubilized form of pig liver b5R[11] served as the template. The FAD-binding domain is drawn in orange, the NADPH-binding domain in blue, FAD in yellow, NADPH in red, and the mutated residues giving rise to methemoglobinemia type I in white. The schematic ribbon diagram was generated with RIBBONS.[57]

The nicotinamide ring was modeled in the *anti* conformation, consistent with the proposed stereochemistry of A-hydrogen transfer in the FNR family.[26] The pyrophosphate moiety is located near the 175 to 190 sequence of the single βα unit of the dinucleotide-binding fold, whereas the 2-OH ribose of NADH interacts in the model with the negatively charged D214. NADH-dependent proteins with a typical dinucleotide fold[58] carry also a negatively charged residue at a similar position to contact the 2-OH of NADH.

Table 3. Mutations in cytochrome b_5 reductase

Amino acid substitution	Reference
Type I mutations	
R49Q	This article
R57Q	33, 35
P64L	This article
L72P	37
P95H	43
V105M	33
P144L	This article
L148P	34, 35
A178V	38
A178T	This article
C203Y	39
E212K	36
L238R	This article
V252M	This article
Type II mutations	
Y42stop	43
R83stop	38
Intron 4 g − 1 → a (skip exon 5)	This article
S127P	31-33
Intron 5 g + 8 → c (skip exon 5)	42
Intron 5 a − 2 → c (skip exon 6)	44
C203R	42
R218stop	42
Intron 8 g − 1 → t (skip exon 9)	41
Deletion M272	42
Deletion F298	40

Single-letter amino acid codes used.

Downloaded from http://ashpublications.net/blood/article-pdf/97/4/1106/1671579/h8040101106.pdf by guest on 02 June 2024

Discussion

In 7 families with methemoglobinemia type I, characterized by cyanosis as the only clinical symptom, we found 6 different missense mutations in *DIA1*, the gene encoding human cytochrome b_5 reductase. These mutations predict amino acid substitutions at various sites in the protein (Table 3). In addition, we found one splice site mutation, which caused skipping of exon 5. This out-of-frame exon skipping in itself leads to enzyme inactivation and type II methemoglobinemia,[42] but in our patient, this mutation was present in heterozygous form, in combination with a L238R substitution. We presume, therefore, that this last amino acid substitution does not have a strong deleterious effect on the b5R activity, because the patient did not suffer from type II symptoms (developmental and neurologic aberrations). Likewise, in family Am, we found 2 compound heterozygous individuals for R49Q and P64L substitutions. Because these patients had very mild cyanotic symptoms, we presume again that these mutations, too, should be classified as type I mutations. The other 3 amino acid substitutions found by us were expressed in homozygous form in type I patients.

In the literature, 7 additional amino acid substitutions have been reported in patients with type I methemoglobinemia[33-39] (Table 3). Some of these mutant enzymes have been expressed in bacterial systems, purified and studied for kinetic properties, heat stability, and trypsin sensitivity.[33,34,38,39] In general, the recombinant type I mutant enzymes were found to have retained about 60% to 70% of the catalytic activity expressed by the recombinant wild-type enzyme, but to be more heat labile and trypsin sensitive. Similar experiments have been carried out with mutant enzymes from patients with type II methemoglobinemia.[32,33,43,59] These enzymes were found to express very low catalytic activity and to be heat labile as well. According to these principles, the P95H mutation studied by Manabe and coworkers,[43] although found in a type II patient, should be classified as a type I mutation, because the recombinant enzyme showed about 60% of the wild-type activity. The patient was a compound heterozygote for this mutation in combination with a Y42stop mutation. Apparently, this combination did not leave enough enzyme activity in the tissues to prevent psychomotor and neurologic deficiencies. Arbitrarily, we have listed this mutation in Table 3 as a type I mutation.

Localization and implication of amino acid substitutions in b5R

Inspection of the 3-dimensional model of b5R (Figure 4) revealed that the amino acid substitutions in b5R of the methemoglobinemia type I patients described in this paper are spread throughout the structure and not directly involved in FAD or NADH binding. The R49Q replacement identified in family Am from Spain concerns a nonconservative mutation located near the protein surface in the first β-strand of the FAD domain. In 1ndh, the Nζof the corresponding K21 forms a strong hydrogen bond with the carbonyl oxygen of the conserved E103.[11] From this observation and the low levels of b5R in family Am we conclude that a positively charged residue at position 49 in human b5R is important for the structural integrity of the FAD-binding domain by forming optimal intradomain contacts.

The P64L substitution, also found in family Am, is localized in a surface loop connecting the first 2 β-strands of the FAD-binding domain. P64 is conserved in 1ndh (P36) and is responsible for the sharp turn of the surface loop comprising residues 62 to 76.[11] On this basis and the very mild cyanotic symptoms in these patients we propose that substitution of P64 influences the folding properties of the FAD-binding domain. As reviewed recently,[60] differences in loop flexibility may lead to a significantly decreased protein stability.

The P144L substitution present in b5R of some members of family W is situated at the C-terminal end of the final β-strand of the FAD-binding domain. This strand is connected by a short loop to the NADH-binding domain. P144 is conserved in 1ndh (P116), solvent accessible and rather far away from the active site.[11] We conclude that the P144L replacement may lead to more conformational freedom impairing optimal interdomain contacts.

The A178T substitution in family O is localized at the C-terminal end of strand β8 of the NADH domain and fairly close to the adenosine moiety of the NADH coenzyme (Figure 4). Although not directly involved in coenzyme recognition, introduction of a bulkier and polar residue at position 178 might influence NADH binding, resulting in decreased catalytic activity.

The L238R substitution in family L from Hong Kong is localized at the C-terminal end of strand 10 of the NADH binding domain, somewhat remote from the protein surface and relatively far away from the domain interface. In 1ndh, L238 is conservatively replaced by a less bulky hydrophobic residue (V210). In the structure of the pig liver enzyme, V210 is relatively close (4 Å) to W217, which is conserved in the human enzyme (W245). Introduction of the polar, bulky arginine side chain at position 238 in human b5R might lead to an electrostatic interaction with E212 (b5R numbering), which is located in the surface loop, connecting strand β9 and helix α3 of the NADH domain. It is conceivable that such an interaction would lead to local structural perturbations, decreasing the overall protein stability.

The V252M substitution found in family V, family A, and Mr T is localized near the protein surface at the end of the large surface loop connecting strand β10 and the short helix α5 of the NADH domain. The side chain of Val 252 is rather close to the amide oxygen of the conserved Asn258 of helix α5 (4.1 Å). Replacement of valine with the bulkier methionine at position 252 might lead to some steric constraints, impairing optimal intradomain contacts.

Previously found amino acid substitutions

As noted above, 8 other type I disease mutations have been found in the b5R gene (Table 3). These mutations are also spread throughout the protein structure and are mostly localized in surface loops. Based on our 3-dimensional model, new insights about some of these mutations are discussed below.

The L72P replacement identified in a Chinese patient[37] is localized in a loop connecting strands β2 and β3 of the FAD domain. This is in disagreement with Wu and colleagues,[37] who concluded that the conserved L72 is part of a β-sheet. The side chain of L72 points toward the inner part of the protein into a hydrophobic environment. Therefore, the L72P replacement might distort the rigidity of the loop, resulting in a decreased stability of the folded protein.

Based on sequence alignments, it was predicted that V105 is part of a β-barrel structure.[33] However, our 3-dimensional model suggests that the V105M replacement identified in a patient from Italy[33] is localized in a loop that connects strands β4 and β5 of the FAD domain. The side chain of V105 is shielded from solvent and is likely involved in maintaining local hydrophobic contacts.

Based on secondary structure analysis, it was predicted that the E212K replacement identified in an African American patient disrupts an α-helix peptide structure.[36] However, our 3-dimensional model suggests that E212 is located in a short surface loop connecting strand β9 and helix α3 of the NADH domain and that

Downloaded from http://ashpublications.net/blood/article-pdf/97/4/1106/1671579/h8040101106.pdf by guest on 02 June 2024

its side chain interacts with the conserved R218. This ionic interaction likely determines the rigidity of the loop.

In conclusion, we have shown that the novel point mutations in the b5R gene of patients with methemoglobinemia result in amino acid replacements that are distributed throughout the protein structure and not in positions directly involved in FAD and NADH binding. This is in agreement with the mild cyanotic symptoms of these patients and supports the idea that enzyme inactivation is a cause of the type II disease, whereas enzyme instability may lead to the type I form. Moreover, from our 3-dimensional model of human b5R, which was constructed on the basis of the crystal structure of the pig liver enzyme,[11] the effects of some other point mutations could be reinterpreted in a rational way. This knowledge, together with additional information on the interaction between b5R and its physiologic electron acceptor cytochrome b_5[61-63] sheds more light on the molecular aspects of methemoglobin reductase deficiency.

References

1. Yubisui T, Takeshita M. Characterization of the purified NADH-cytochrome b5 reductase of human erythrocytes as a FAD containing enzyme. J Biol Chem. 1980;255:2454-2456.
2. Oshino N, Imai Y, Sato R. A function of cytochrome b5 in fatty acid desaturation by rat liver microsomes. J Biochem (Tokyo). 1971;69:155-167.
3. Keyes SR, Cinti DL. Biochemical properties of cytochrome b5-dependent microsomal fatty acid elongation and identification of products. J Biol Chem. 1980;255:11357-11364.
4. Reddy VVR, Kupfer D, Capsi E. Mechanism of C-5 double bond introduction in the biosynthesis of cholesterol by rat liver microsomes: evidence for the participation of microsomal cytochrome b5. J Biol Chem. 1977;252:2797-2801.
5. Hildebrandt A, Estabrook RW. Evidence for the participation of cytochrome b5 in hepatic microsomal mixed-function oxidation reactions. Arch Biochem Biophys. 1971;143:66-79.
6. Hultquist DE, Passon PG. Catalysis of methaemoglobin reduction by erythrocyte cytochrome b5 and cytochrome b5 reductase. Nat New Biol. 1971;229:252-254.
7. Yubisui T, Miyata T, Iwanaga S, Tamura M, Takeshita M. Complete amino acid sequence of NADH-cytochrome b5 reductase purified from human erythrocytes. J Biochem (Tokyo). 1986; 99:407-422.
8. Tomatsu S, Kobayashi Y, Fukumaki Y, Yubisui T, Orii T, Sakaki Y. The organization and the complete nucleotide sequence of the human NADH cytochrome b5 reductase gene. Gene. 1989;80: 353-361.
9. Bulbarelli A, Valentini A, De Silvestris M, Cappellini MD, Borgese N. An erythroid-specific transcript generates the soluble form of NADH-cytochrome b5 reductase in humans. Blood. 1998;92:310-319.
10. Pietrini G, Carrera P, Borgese N. Two transcripts encode rat cytochrome b5 reductase. Proc Natl Acad Sci U S A. 1988;85:7246-4250.
11. Nishida H, Inaka K, Yamanaka M, Kaida S, Kobayashi K, Miki K. Crystal structure of NADH cytochrome b5 reductase from pig liver at 2.4 Å resolution. Biochemistry. 1995;34:2763-2767.
12. Takano T, Bando S, Horri, Higashiyama M, et al. The structure of human erythrocyte NADH-cytochrome b5 reductase at 2.5Å resolution. In: Yagi K, ed. Flavins and Flavoproteins. Berlin: Walter de Gruyter; 1994:409-412.
13. Karplus PA, Daniels MJ, Herriott JR. Atomic structure of ferredoxin-NADP+ reductase: prototype for a structurally novel flavoenzyme family. Science. 1991;251:60-66.
14. Rossmann MG, Moras D, Olsen KW. Chemical and biological evolution of a nucleotide-binding protein. Nature. 1974;250:194-199.
15. Porter TD, Kasper CB. NADPH-cytochrome P-450 oxidoreductase: flavin mononucleotide and flavin adenine dinucleotide domains evolved from different flavoproteins. Biochemistry. 1986;25: 1682-1687.
16. Crawford NM, Smith M, Belissimo D, Davis RW. Sequence and nitrate regulation of the *Arabidopsis thaliana* mRNA encoding nitrate reductase, a metalloflavoprotein with three functional domains. Proc Natl Acad Sci U S A. 1988;85:5006-5010.
17. Sutter TR, Sanglard D, Loper JC. Isolation and characterization of the alkane-inducible NADPH-cytochrome P-450 oxidoreductase gene from *Candida tropicalis*: identification of invariant residues within similar amino acid sequences of divergent flavoproteins. J Biol Chem. 1990;265: 16428-16436.
18. Hyde GE, Crawford NM, Campbell WH. The sequence of squash NADH:nitrate reductase and its relationship to the sequences of other flavoprotein oxidoreductases. J Biol Chem. 1991;266: 23542-23547.
19. Correll CC, Ludwig ML, Bruns CM, Karplus PA. Structural prototypes for an extended family of flavoprotein reductases: comparison of phthalate dioxygenase reductase with ferredoxin reductase and ferredoxin. Protein Sci. 1993;2:2112-2133.
20. Lu G, Campbell WH, Schneider G, Lindqvist Y. Crystal structure of the FAD-containing fragment of corn nitrate reductase at 2.5 Å resolution: relationship to other flavoprotein reductases. Structure. 1994;2:809-821.
21. Bruns CM, Karplus PA. Refined crystal structure of spinach ferredoxin reductase at 1.7 Å resolution: oxidized, reduced and 2′-phospho-5′-AMP bound states. J Mol Biol. 1995;247:125-145.
22. Nishida H, Inaka K, Miki K. Specific arrangement of three amino acid residues for flavin-binding barrel structures in NADH-cytochrome b5 reductase and the other flavin-dependent reductases. FEBS Lett. 1995;361:97-100.
23. Serre L, Vellieux FMD, Medina M, Gomez-Moreno C, Fontecilla-Camps JC, Frey M. X-ray structure of the ferredoxin NADP reductase from the cyanobacterium *Anabaena* PCC 7119 at 1.8 Å resolution and crystallographic studies of NADP binding at 2.25 Å resolution. J Mol Biol. 1996;263:20-39.
24. Wang M, Roberts DL, Paschke R, Shea TM, Masters BSS, Kim J-JP. Three-dimensional structure of NADPH-cytochrome P450 reductase: prototype for FMN- and FAD-containing enzymes. Proc Natl Acad Sci U S A. 1997;94:8411-8416.
25. Sridhar Prasad G, Kresge N, Muhlberg AB, et al. The crystal structure of NADPH:ferredoxin reductase from *Azotobacter vinelandii*. Protein Sci. 1998;7:2541-2549.
26. Deng Z, Aliverti A, Zanetti G, et al. A productive NADP+ binding mode of ferredoxin-NADP+ reductase revealed by protein engineering and crystallographic studies. Nat Struct Biol. 1999;6: 847-853.
27. Gibson QH. The reduction of methaemoglobin in red blood cells and studies on the cause of idiopathic methaemoglobinaemia. Biochem J. 1948; 42:13.
28. Scott EM, Griffith IV. The enzymic defect of hereditary methemoglobinemia: diaphorase. Biochim Biophys Acta. 1959;34:584-586.
29. Worster-Drought C, White JC, Sargent F. Familial, idiopathic methaemoglobinaemia associated with mental deficiency and neurological abnormalities. Br Med J. 1953;2:114-118.
30. Leroux A, Junien C, Kaplan J-C, Bamberger J. Generalized deficiency of cytochrome b5 reductase in congenital methaemoglobinaemia with mental retardation. Nature. 1975;258:619-620.
31. Kobayashi Y, Fukumaki Y, Yubisui T, Inoue J, Sakaki Y. Serine-proline replacement at residue 127 of NADH-cytochrome b5 reductase causes hereditary methemoglobinemia, generalized type. Blood. 1990;75:1408-1413.
32. Yubisui T, Shirabe K, Takeshita M, et al. Structural role of serine 127 in the NADH-binding site of human NADH-cytochrome b5 reductase. J Biol Chem. 1991;266:66-70.
33. Shirabe K, Yubisui T, Borgese N, Tang CY, Hultquist DE, Takashita M. Enzymatic instability of NADH-cytochrome b5 reductase as a cause of hereditary methemoglobinemia type I (red cell type). J Biol Chem. 1992;267:20416-20421.
34. Nagai T, Shirabe K, Yubisui T, Takeshita M. Analysis of mutant NADH-cytochrome b5 reductase: apparent "type III" methemoglobinemia can be explained as type I with an unstable reductase. Blood. 1993;81:808-814.
35. Katsube T, Sakamoto N, Kobayashi Y, et al. Exonic point mutations in NADH cytochrome b5 reductase genes of homozygotes for hereditary methemoglobinemia, types I and III: putative mechanisms of tissue-dependent enzyme deficiency. Am J Hum Genet. 1991;48:799-808
36. Jenkins MM, Prchal JF. A novel mutation in the 3′domain of NADH-cytochrome b5 reductase in an African-American family with type I congenital methemoglobinemia. Blood. 1996;87:2993-2999.
37. Wu YS, Huang CH, Wan Y, Huang QJ, Zhu Zy. Identification of a novel point mutation (Leu72→Pro) in the NADH-cytochrome b5 reductase gene of a patient with hereditary methaemoglobinaemia type I. Br J Haematol. 1998;102:575-577.
38. Higasa K, Manabe JI, Yubisui T, et al. Molecular basis of hereditary methaemoglobinaemia, types I and II: two novel mutations in the NADH-cytochrome b5 reductase gene. Br J Haematol. 1998;103:922-930.
39. Wang Y, Wu YS, Zheng PZ, et al. A novel mutation in the NADH-cytochrome b5 reductase gene of a Chinese patient with recessive congenital methemoglobinemia. Blood. 2000;95:3250-3255.
40. Shirabe K, Fujimoto Y, Yubisui T, Takeshita M. An in-frame deletion of codon 298 of the NADH-cytochrome b5 reductase gene results in hereditary methemoglobinemia type II (generalized type). A functional implication for the role of the COOH-terminal region of the enzyme. J Biol Chem. 1994;269:5952-5957.
41. Shirabe K, Landi MT, Takeshita M, Uziel G, Fedrizzi E, Borgese N. A novel point mutation in a 3′splice site of the NADH-cytochrome b5 reductase gene results in immunologically undetectable enzyme and impaired NADH-dependent ascorbate regeneration in cultured fibroblasts of a patient with type II hereditary methemoglobinemia. Am J Hum Genet. 1995;57:302-310.
42. Mota Vieira L, Kaplan J-C, Kahn A, Leroux A. Four new mutations in the NADH-cytochrome b5 reductase gene from patients with recessive congenital methemoglobinemia type II. Blood. 1995; 85:2254-2262.
43. Manabe J, Arya R, Sumimoto H, et al. Two novel

Downloaded from http://ashpublications.net/blood/article-pdf/97/4/1106/1671579/h8040101106.pdf by guest on 02 June 2024

mutations in the reduced nicotinamide adenine dinucleotide (NADH)-cytochrome b5 reductase gene of a patient with generalized type, hereditary methemoglobinemia. Blood. 1996;88:3208-3215.

44. Owen EP, Berens J, Marinaki AM, Ipp H, Harley EH. Recessive congenital methaemoglobinaemia type II, a new mutation which causes incorrect splicing in the NADH-cytochrome b5 reductase gene. J Inher Metab Dis. 1997;20:610.
45. Hegesh E, Calmanovici N, Avron M. New method for determining ferrihemoglobin reductase (NADH-methemoglobin reductase) in erythrocytes. J Lab Clin Med. 1968;72:339-344.
46. Evelyn KA , Malloy HT. Microdetermination of oxyhemoglobin, methemoglobin, and sulfhemoglobin in a single sample of blood. J Biol Soc. 1938;126:655-662.
47. Chirgwin JM, Przybyla AE, MacDonald RJ, Rutter WJ. Isolation of biologically active ribonucleic acid from sources enriched in ribonuclease. Biochemistry. 1979;18:5294-5299.
48. Bolscher BGJM, de Boer M, de Klein A, Weening RS, Roos D. Point mutations in the b-subunit of cytochrome b558 leading to X-linked chronic granulomatous disease. Blood. 1991;77:2482-2487.
49. Sali A, Blundell TL. Comparative protein modeling by satisfaction of spacial restraints. J Mol Biol. 1993;234:779-815.
50. Brooks BR, Bruccoleri RE, Olafson BD, States DJ, Swiminathan S, Karplus M. CHARMM, a program for macromolecular energy minimization and dynamics calculations. J Comp Chem. 1983; 4:187-217.
51. Laskowski RA, McArthur MW, Moss DS, Thornton JM. PROCHECK: a program to check the stereochemical quality of protein structures. J Appl Crystallogr. 1993;26:283-291.
52. Lüthy R, Bowie JU, Eisenberg D. Assessment of protein models with three-dimensional profiles. Nature. 1992;356:83-85.
53. Sippl MJ. Recognition of errors in three-dimensional structures of proteins. Proteins. 1993;17:355-362.
54. Brünger AT. X-plor, version 3.1, a system for the X-ray crystallography and NMR. New Haven, CT: Yale University Press; 1992.
55. Jones TA, Zou J-Y, Cowan S, Kjeldgaard M. Improved methods for the building of protein models in electron density maps and the location of errors in these models. Acta Crystallogr Sect A. 1991;47:110-119.
56. Leusen JHW, Meischl C, Eppink MHM, et al. Four novel mutations in the gene encoding gp91-phox of human NADPH oxidase: consequences for oxidase assembly. Blood. 2000;95:666-673.
57. Carson M. Ribbons 2.0. J Appl Crystallogr. 1991; 24: 958-961.
58. Lesk AM. NAD-binding domains of dehydrogenases. Curr Opin Struct Biol. 1995;5:775-783.
59. Shirabe K, Yubusui T, Nishino T, Takeshita M. Role of cysteine residues in human NADH-cytochrome b5 reductase studied by site-directed mutagenesis. J Biol Chem. 1991;266:7531-7336.
60. Dobson CM, Karplus M. The fundamentals of protein folding: bringing together theory and experiment. Curr Opin Struct Biol. 1999;9:92-101.
61. Nishida H, Miki K. Electrostatic properties deduced from refined structures of NADH cytochrome b5 reductase and the other flavin-dependent reductases: pyridine nucleotide binding and interaction with an electron transfer partner. Proteins. 1996;26:32-41.
62. Shirabe K, Nagai T, Yubisui T, Takeshita M. Electrostatic interaction between NADH-cytochrome b5 reductase and cytochrome b5 studied by site-directed mutagenesis. Biochim Biophys Acta. 1998;1384:16-22.
63. Kawano M, Shirabe K, Nagai T, Takeshita M. Role of carboxyl residues surrounding the heme of human cytochrome b5 in the electrostatic interaction with NADH cytochrome b5 reductase. Biochem Biophys Res Commun. 1998;245:666-669.

Downloaded from http://ashpublications.net/blood/article-pdf/97/4/1106/1671579/h8040101106.pdf by guest on 02 June 2024